Delft University of Technology

Attribution of extreme rainfall from Hurricane Harvey, August 2017

Van Oldenborgh, Geert Jan; Van Der Wiel, Karin; Sebastian, A.G.; Singh, Roop; Arrighi, Julie; Otto, Friederike; Haustein, Karsten; Li, Sihan; Vecchi, Gabriel; Cullen, Heidi

LETTER • OPEN ACCESS

Attribution of extreme rainfall from Hurricane Harvey, August 2017

To cite this article: Geert Jan van Oldenborgh *et al* 2017 *Environ. Res. Lett.* **12** 124009

View the article online for updates and enhancements.

Environmental Research Letters

CORRIGENDUM

Corrigendum: Attribution of extreme rainfall from Hurricane Harvey, August 2017 (2017 *Environ. Res. Lett.* **12** 124009)

Geert Jan van Oldenborgh[1,8] , Karin van der Wiel[1] , Antonia Sebastian[2,3] , Roop Singh[4], Julie Arrighi[4] , Friederike Otto[5] , Karsten Haustein[5] , Sihan Li[5] , Gabriel Vecchi[6] and Heidi Cullen[7]

1   Royal Netherlands Meteorological Institute (KNMI), R&D Weather and Climate Models, De Bilt, Netherlands
2   Faculty of Civil Engineering and Geosciences, Delft University of Technology, Delft, Netherlands
3   Department of Civil and Environmental Engineering, Rice University, Houston, TX, United States of America
4   Red Cross Red Crescent Climate Centre, The Hague, Netherlands
5   School of Geography and the Environment and Department of Physics, University of Oxford, Oxford, United Kingdom
6   Princeton University, Princeton, NJ, United States of America
7   Climate Central, Princeton, NJ, United States of America
8   Author to whom any correspondence should be addressed.

E-mail: oldenborgh@knmi.nl

Updated EC-Earth results

In the computation of the EC-Earth results, we accidentally included all grid boxes and not only the land points as we intended. We redid the calculations using the land points only. This implies an update to figure 6 (given below), but it makes only a slight differences to the EC-Earth results. The comparison with the observed fit for the model evaluation is somewhat better in the dispersion parameter σ/μ and now good in the shape parameter, although the model now requires a bias correction of 18%. The increase in intensity for land points only is $\Delta I = 17\%$ (11% ... 23%), compared to the $\Delta I = 17\%$ (10% ... 23%) for all points. The risk ratio is a bit higher, 2.5 (1.8 ... 6.7) instead of the 2.2 (1.5 ... 4.1) reported in the article.

Updated synthesis and conclusions

This changes figure 7 slightly as well, but does not affect the conclusions. The change in increase remains 15% with an uncertainty range 8%–19%. The change in risk ratio stays the same, a factor of three, but with a slightly higher uncertainty range, 1.6–6 rather than 1.5–5. This strengthens our conclusions by a negligible factor.

ORCID iDs

Geert Jan van Oldenborgh https://orcid.org/0000-0002-6898-9535
Karin van der Wiel https://orcid.org/0000-0001-9365-5759
Antonia Sebastian https://orcid.org/0000-0002-4309-2561
Julie Arrighi https://orcid.org/0000-0003-4714-4514
Friederike Otto https://orcid.org/0000-0001-8166-5917
Karsten Haustein https://orcid.org/0000-0003-3126-7851
Sihan Li https://orcid.org/0000-0002-2479-8665
Gabriel Vecchi https://orcid.org/0000-0002-5085-224X
Heidi Cullen https://orcid.org/0000-0002-6976-2631
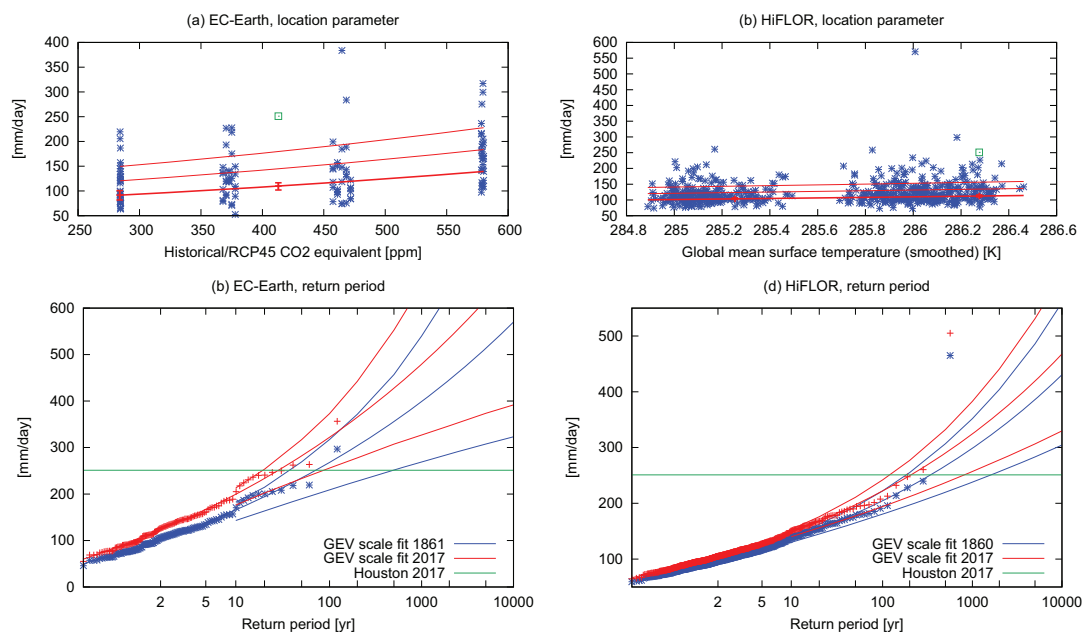
Figure 6. The same as figure 4, but for (*a*)–(*c*) the four EC-Earth T799 experiments and (*b*)–(*d*) the four static forcing HiFLOR experiments. For EC-Earth, the fit of the annual and spatial maximum three-day average precipitation on the US Gulf Coast to a GEV that scales with the RCP4.5 equivalent CO_2 concentration. For HiFLOR, the fit is to a GEV that scales with the modelled GMST.

Figure 7. Synthesis of the results. (*a*) Intensity changes 1880–2017 for local and regional extreme three-day precipitation events along the US Gulf Coast (%). Observations are shown in blue, models in red. The magenta line is the average of the three estimates from local observations (with smaller uncertainties) and the two regional model analyses (that can only reproduce these more extreme events reliably). (*b*) Same for the risk ratios (changes in probability).

Environmental Research Letters

LETTER

Attribution of extreme rainfall from Hurricane Harvey, August 2017

Geert Jan van Oldenborgh[1,8] ⓘ, Karin van der Wiel[1] ⓘ, Antonia Sebastian[2,3] ⓘ, Roop Singh[4], Julie Arrighi[4] ⓘ, Friederike Otto[5] ⓘ, Karsten Haustein[5] ⓘ, Sihan Li[5] ⓘ, Gabriel Vecchi[6] ⓘ and Heidi Cullen[7] ⓘ

1   Royal Netherlands Meteorological Institute (KNMI), R&D Weather and Climate Models, De Bilt, The Netherlands
2   Faculty of Civil Engineering and Geosciences, Delft University of Technology, Delft, The Netherlands
3   Department of Civil and Environmental Engineering, Rice University, Houston, TX, United States of America
4   Red Cross Red Crescent Climate Centre, The Hague, The Netherlands
5   School of Geography and the Environment and Department of Physics, University of Oxford, Oxford, United Kingdom
6   Princeton University, Princeton, NJ, United States of America
7   Climate Central, Princeton, NJ, United States of America
8   Author to whom any correspondence should be addressed.

E-mail: oldenborgh@knmi.nl

Keywords: extreme precipitation, tropical cyclone, attribution, climate change

Supplementary material for this article is available online

Abstract

During August 25–30, 2017, Hurricane Harvey stalled over Texas and caused extreme precipitation, particularly over Houston and the surrounding area on August 26–28. This resulted in extensive flooding with over 80 fatalities and large economic costs. It was an extremely rare event: the return period of the highest observed three-day precipitation amount, 1043.4 mm 3dy^{-1} at Baytown, is more than 9000 years (97.5% one-sided confidence interval) and return periods exceeded 1000 yr (750 mm 3dy^{-1}) over a large area in the current climate. Observations since 1880 over the region show a clear positive trend in the intensity of extreme precipitation of between 12% and 22%, roughly two times the increase of the moisture holding capacity of the atmosphere expected for 1 °C warming according to the Clausius–Clapeyron (CC) relation. This would indicate that the moisture flux was increased by both the moisture content and stronger winds or updrafts driven by the heat of condensation of the moisture. We also analysed extreme rainfall in the Houston area in three ensembles of 25 km resolution models. The first also shows 2 × CC scaling, the second 1 × CC scaling and the third did not have a realistic representation of extreme rainfall on the Gulf Coast. Extrapolating these results to the 2017 event, we conclude that global warming made the precipitation about 15% (8%–19%) more intense, or equivalently made such an event three (1.5–5) times more likely. This analysis makes clear that extreme rainfall events along the Gulf Coast are on the rise. And while fortifying Houston to fully withstand the impact of an event as extreme as Hurricane Harvey may not be economically feasible, it is critical that information regarding the increasing risk of extreme rainfall events in general should be part of the discussion about future improvements to Houston's flood protection system.

1. Introduction

Hurricane Harvey formed as a tropical storm over the Atlantic Ocean on August 17, 2017 and crossed into the Caribbean Sea the next day. It weakened to a tropical depression as it crossed the Yucatan Peninsula, but attained hurricane strength over the Gulf of Mexico on August 24, rapidly intensifying to reach

Category 4 strength just before making landfall on the Texas coast 50 km east of Corpus Christi on August 25, causing severe wind damage in coastal towns. Harvey moved slowly inland, remaining nearly stationary about 100 km inland for four days before moving back into the Gulf and making a second landfall in Louisiana on August 30. While Hurricane Harvey was a significant hurricane in terms of its size and wind speed,

ultimately, the storm will be remembered for the extreme flooding it caused in Houston and surrounding areas.

Between August 25–30, unprecedented rainfall totals for a tropical cyclone (TC) in the contiguous United States were recorded. The station Cedar Bayou at FM1942 (www.harriscountyfws.org/GageDetail/Index/1730), about 40 km west of Houston, had observed an accumulated 1318 mm (51.89″) by Thursday August 31, 10 AM CDT. Widespread flooding necessitated more than 120 000 rescues, exceeding the capacity of formal emergency response organisations and requiring the assistance of volunteers with access to boats or large vehicles. Over 80 deaths have been attributed to Harvey, mostly as a result of drowning, and financial analysts estimate it to be among the costliest natural disaster in US history (NOAA NCEI 2017). It is estimated that flooding ultimately impacted more than 100 000 homes, of which nearly 80 000 are estimated to have been flooded to a depth of at least 0.46 m (18″) and 23 000 to at least 1.5 m (5 ft) (FEMA 2017).

In the immediate aftermath of the event, the question was raised as to what extent the impacts of Hurricane Harvey were intensified due to anthropogenic climate change. In this paper, we analyze the rainfall associated with Hurricane Harvey, contextualising it with relevant flood risk factors, to answer this question.

The observed and expected response of TCs to greenhouse gas-induced climate change has been the subject of intense research. Globally, there is an expectation that increasing greenhouse gases will lead to a decrease or no change in the overall number of TCs, but that the maximum wind speed and precipitation of the strongest storms should increase (Hesselbjerg Christensen *et al* 2013). However, there is low confidence in region-specific projections. For the Atlantic basin, there is considerable spread in the expected change in TC frequency resulting from CO_2 increases, even considering only the strongest storms (Knutson *et al* 2013). Furthermore, changes in observing practices limit confidence in century-scale trends in Atlantic hurricane frequency (Vecchi and Knutson, 2011). That is, at this stage, there is no clear scientific evidence to support the notion that the existence of Harvey was made more likely by global warming.
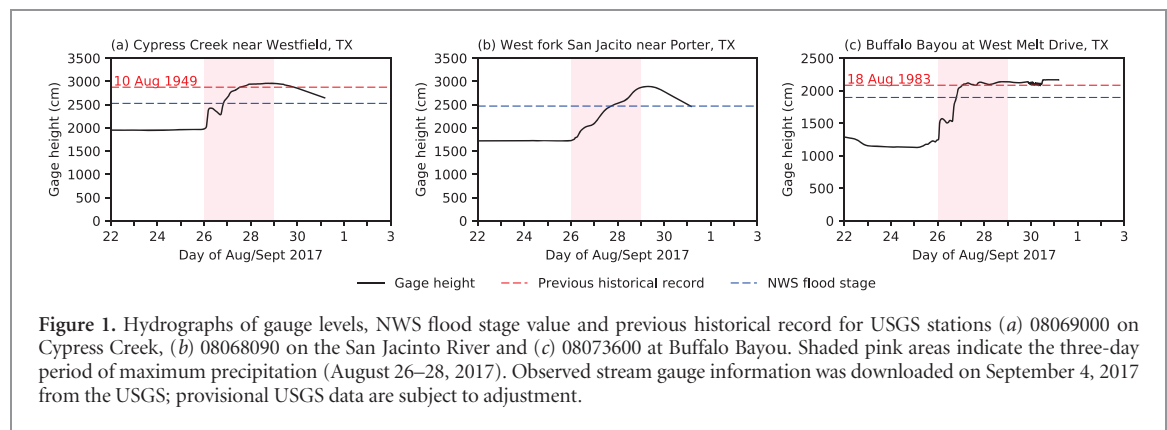
However, the impacts of Harvey may have been influenced by global warming; studies consistently indicate that greenhouse gas-induced warming should lead to increases in the total and maximum rainfall by TCs (Knutson *et al* 2010, Scoccimarro *et al* 2014, Villarini *et al* 2014). In general, the maximum moisture content of air increases with 6%–8.5% per degree warming, according to the Clausius-Clapeyron (CC) relationship (Clapeyron 1834, Clausius 1850, Held and Soden 2006, O'Gorman 2015). If relative humidity stays the same, which is the norm near oceans, the actual amount of water vapour in the air increases by the same amount. Studies exploring the response of TC rainfall to greenhouse warming find rates of increase at least as large as CC-scaling, with various studies indicating increases that follow or exceed CC-scaling (e.g. Knutson *et al* 2010, 2013, Scoccimarro *et al* 2014). The hypothesis underlying higher scaling is that the extra heat of condensation gives extra energy to drive the circulation in a well-organised system. The moisture flux is thus enhanced twice: not only with higher moisture content, but also with higher velocities. This could result in up to two times CC-scaling, as was found on smaller and shorter time scales by Lenderink *et al* (2017). Another contribution may be a possible increase in the probability that a hurricane stalls over the coast either by a systematic trend in persistency of high pressure events globally (Mann *et al* 2017) or simply a local tendency in mean circulation.

Van der Wiel *et al* (2017) showed that the high tail of the distribution of extreme precipitation on the US Gulf Coast can be described well by a generalised extreme value distribution (GEV), in spite of the many different mechanisms that cause these high precipitation events there (Schumacher and Johnson 2006). It was found that the change in intensity was compatible with $2 \times CC$ scaling. The distribution of the most extreme events was also found to be simulated reasonably well by the GFDL HiFLOR model with a 25 km atmospheric resolution, and to a lesser extent by the 50 km resolution FLOR-FA model. These models simulated $1 \times CC$ scaling for the most extreme events, as is observed for global one-day precipitation extremes (Westra *et al* 2013). However, regionally and for longer time-scale events, the scaling may well be different. For instance, in Boulder, Colorado, lower scaling was found for five-day precipitation extremes (Hoerling *et al* 2013, Eden *et al* 2016).

We follow the same methodology as van der Wiel *et al* (2017) to attribute the extreme precipitation from Hurricane Harvey to anthropogenic climate change and refer to that paper for an extensive discussion of the methods and assumptions. In addition, we are including two supplementary observational datasets and two additional high-resolution models. This analysis does not consider the relatively low-resolution (50 km) FLOR-FA model.

The analysis herein focuses on extreme precipitation as the primary cause of flooding. We do not consider the backwater effects of elevated water levels due to storm surge or relative sea level rise in Galveston Bay on the ability of the system to drain, but previous studies have suggested that this may be an important factor in determining the intensity and extent of coastal flooding (Torres *et al* 2015, Sebastian *et al* 2017). In addition, we acknowledge that other anthropogenic factors have contributed to increased flood risk in Houston, specifically urban development, which has led to floodplain encroachment, increased impervious cover, reduced overland and channel roughness, decreased storage capacity (Brody *et al* 2008, 2011), and resource withdrawal that has led to

Figure 1. Hydrographs of gauge levels, NWS flood stage value and previous historical record for USGS stations (*a*) 08069000 on Cypress Creek, (*b*) 08068090 on the San Jacinto River and (*c*) 08073600 at Buffalo Bayou. Shaded pink areas indicate the three-day period of maximum precipitation (August 26–28, 2017). Observed stream gauge information was downloaded on September 4, 2017 from the USGS; provisional USGS data are subject to adjustment.

subsidence of up to 3 m (10 ft) (http://hgsubsidence. org/subsidence-data/). Moreover, the operation of emergency flood control structures, such as the Addicks and Barker Reservoirs west of downtown Houston, further exacerbated flooding in some areas of the city. While the impact of urban development and subsidence on flooding during Hurricane Harvey is not directly addressed in this paper, we provide suggestions for future research regarding this event and its impacts.

2. Event definition

The time scale of the event definition is set by the main impact: flooding in the city of Houston. Hydrographs at http://water.weather.gov/ahps/region.php?state=tx show that most rivers and bayous in Houston crested on Monday August 28 or Tuesday August 29 local time, see figures 1(*a*) and (*b*). Note that Buffalo Bayou is an exception, as it was affected by the controlled release of waters from the Addicks and Barker Reservoirs upstream (figure 1(*c*)). The 10 minute meteorological station 'Houston' (ID 639466112 on wow.knmi.nl, figures 2(*a*) and (*b*)) also shows that the three days up to Monday August 28 produced the highest amounts of precipitation. We therefore take the three-day average for Saturday August 26 to Monday August 28 to be the most relevant time scale. This implies the rainfall accumulations we consider are lower than the all-storm totals mentioned in the introduction.

The highest official gauge recording over the three-day period reported immediately after the event was at the William P. Hobby International Airport (Hobby Airport), WMO 72244, with 824.7 mm $3dy^{-1}$ ($32.47''$ $3dy^{-1}$), corresponding to 274.9 mm dy^{-1} ($10.82''$ day^{-1}) on August 26–28. At airports, this is usually 0–24 UTC. Later updates of the GHCN-D v2 dataset added to stations with higher precipitation: Houston NWSO (USC00414333) with 999.2 on August 26–28 and Baytown (USC00410586) with 1043.4 mm $3dy^{-1}$ ($41.07''$ $3dy^{-1}$), corresponding to 347.8 mm dy^{-1} ($13.69''$ dy^{-1}) on August 27–29, presumably 8–8 local time. We use the latter value as the highest observed point value for this event.
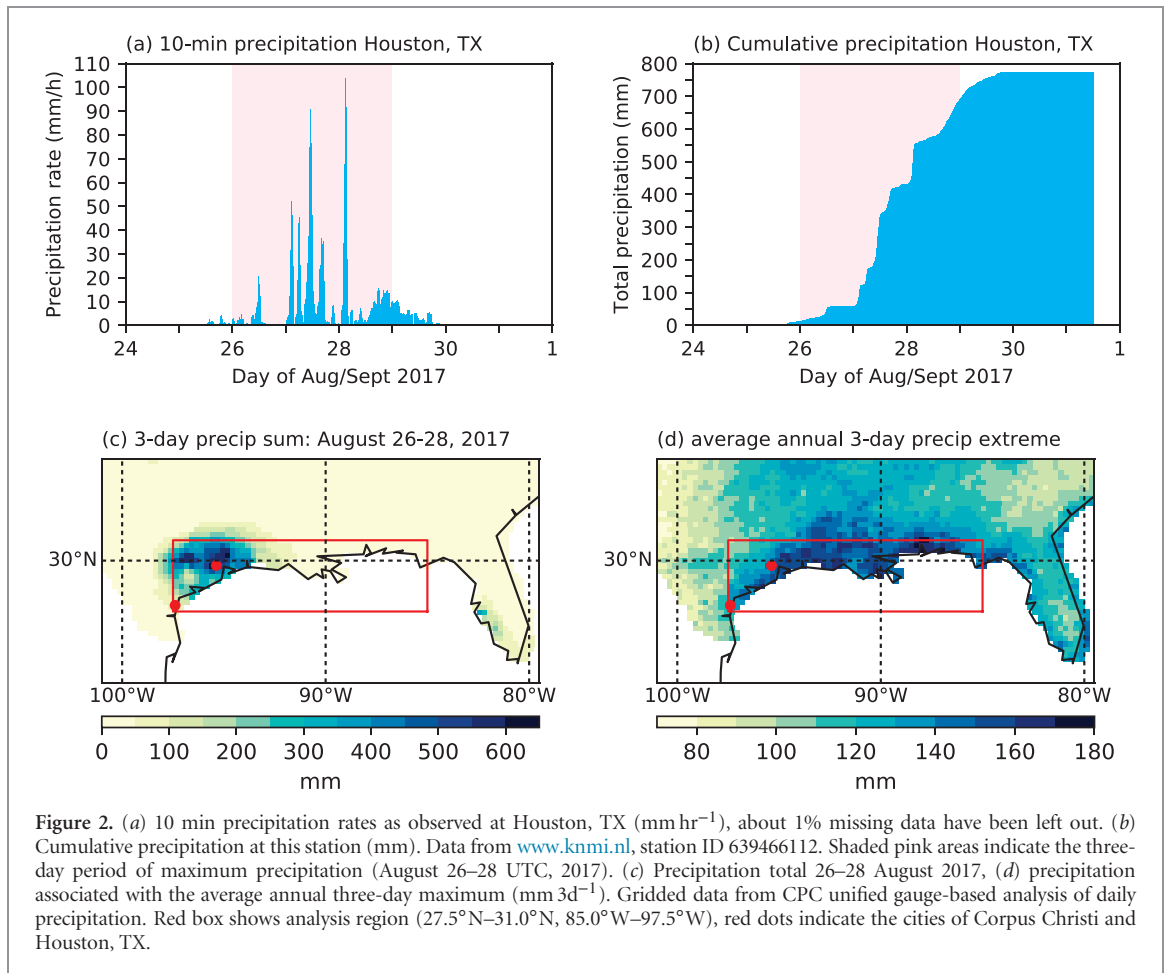
Amateur stations give even higher amounts, but were not used in this study. It should be noted that often-quoted '72 hr sums' use higher resolution data (hourly or 10 minute) and choose the beginning arbitrarily. This precludes comparison with historical observations that are usually daily with a fixed observation time.

Van der Wiel *et al* (2017) showed that extreme precipitation could be considered homogeneous along the Gulf Coast, using the land area 29°N–31°N, 85°W–95°W. As the most-affected areas are just west of this box, we extended it to Corpus Christi, 27.5°N–31°N, 85°W–97.5°W (figures 2(*c*) and (*d*)). The extreme western part of this area has slightly lower extreme precipitation, but this does not affect the analysis, especially not the spatial maximum that is used for the models. Note that extreme precipitation in this area is not only due to tropical storms, but also to a variety of other mechanisms such as the cut-off low studied in van der Wiel *et al* (2017). Extreme precipitation events occur throughout the year, with only a modest increase in the hurricane season (June–November).

3. Data and methods

3.1. Observational data
For the observational analysis, we primarily use the two rain gauge-based datasets that were also used in van der Wiel *et al* (2017). The first is the GHCN-D v2 collection of rain gauge data extended with GTS data. There are 312 stations in the box covering 1878–2017. The density of stations is much higher than the decorrelation length of three-day precipitation. To obtain less-dependent datasets, we analyse the station data in two ways: all stations with 30 or more years of data and at least 0.1° apart (85 stations), and a subset with 80 years or more of data and at least 1° apart (13 stations). The subsetting was done in the order of station IDs. The first subset is slightly stricter than in the previous study (van der Wiel *et al* 2017) to ensure the validity of the moving spatial blocks technique that we use in the bootstrap to obtain uncertainty estimates in the presence of spatial dependencies. We finally note that the rain gauges have varying observation times.

Figure 2. (*a*) 10 min precipitation rates as observed at Houston, TX (mm hr^{-1}), about 1% missing data have been left out. (*b*) Cumulative precipitation at this station (mm). Data from www.knmi.nl, station ID 639466112. Shaded pink areas indicate the three-day period of maximum precipitation (August 26–28 UTC, 2017). (*c*) Precipitation total 26–28 August 2017, (*d*) precipitation associated with the average annual three-day maximum (mm 3d^{-1}). Gridded data from CPC unified gauge-based analysis of daily precipitation. Red box shows analysis region (27.5°N–31.0°N, 85.0°W–97.5°W), red dots indicate the cities of Corpus Christi and Houston, TX.

For comparison against the model data, we use the CPC Unified Precipitation Analysis, a 25 km gridded dataset based on rain gauges. This dataset has a maximum three-day precipitation of 251.1 mm dy^{-1} or 614.2 mm 3dy^{-1} (9.89″ day^{-1} or 24.18″ 3dy^{-1}), see figure 3(*b*). This is only slightly lower than the highest point value available at the time in spite of the area-averaging, showing the large spatial extent of the extreme precipitation. However, the observations at Baytown and Houston NWSO, and a comparison with the rain radar data (figure 3(*c*)), show that this dataset likely underestimated the rainfall. However, as it is the best estimate we have with a long time series, we use it anyway, keeping this underestimation in mind.
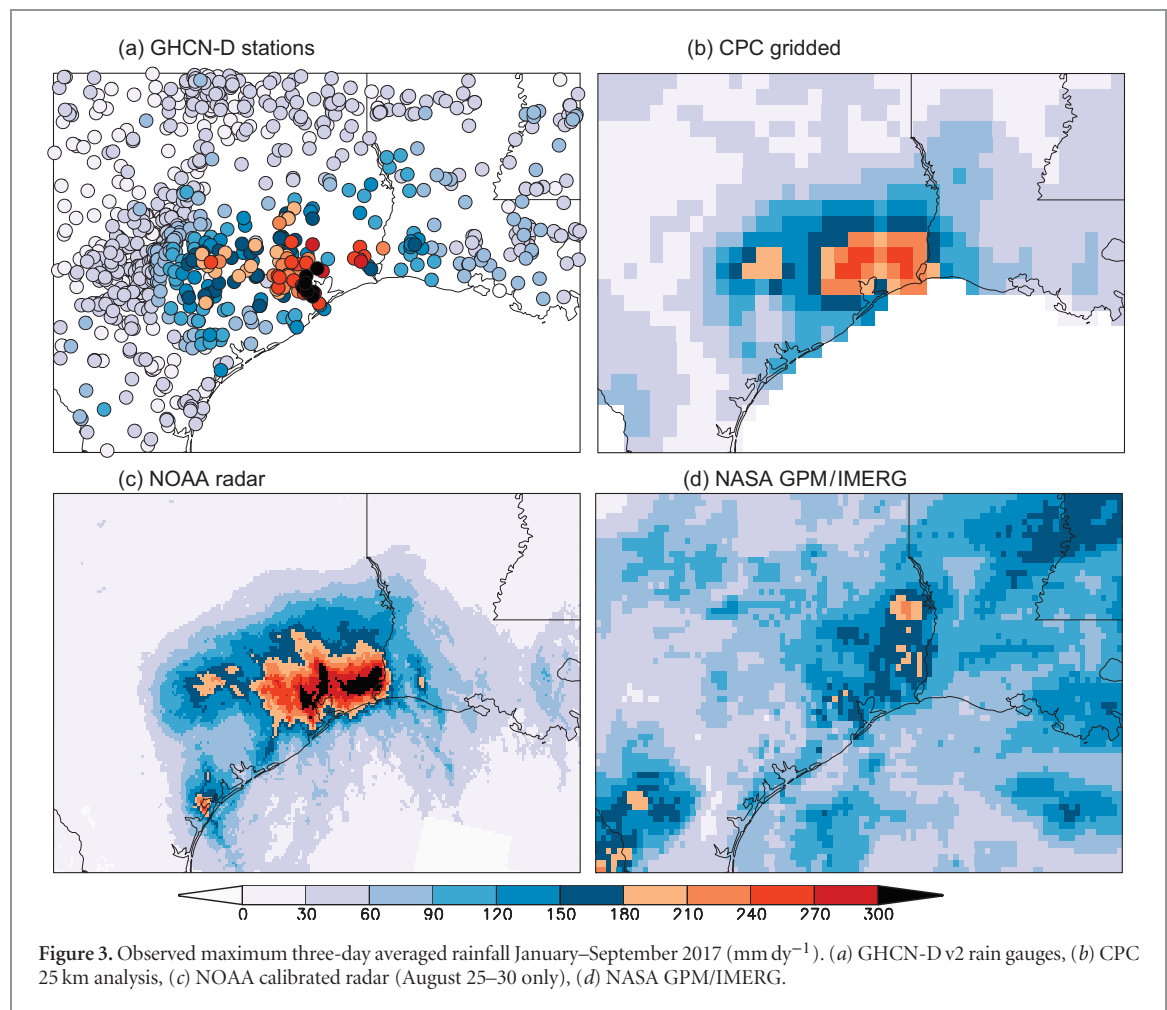
At this resolution, the grid points are insufficiently independent to do an extreme value analysis, so for these we averaged the grid boxes into a 50 km grid. At this resolution the highest 2017 value is 186.7 mm dy^{-1} or 560.2 mm 3dy^{-1} (7.35″ dy^{-1} or 22.05″ 3dy^{-1}).

To check these datasets, we also considered the NASA GPM/IMERG data and the NOAA calibrated rain radar fields. The NASA dataset is 0–24 UTC and the NOAA dataset 12–12 UTC. In figures 3(*c*) and (*d*) we show the highest three-day precipitation in 2017 up to September 30 (only for August 25–30 for NOAA) fields. The NOAA calibrated rain radar dataset has somewhat higher point maxima, up to 385.5 mm dy^{-1} or 1156.5 mm 3dy^{-1} (15.18″ dy^{-1} or 45.53″ 3dy^{-1}), as

it can catch local maxima that usually are not caught by official rain gauges. However, as it has no long historical record, we could not use it for the quantitative analysis. The NASA GPM/IMERG datasets show lower maximum amounts than any other dataset, 203.3 mm dy^{-1} (8.00″ dy^{-1}) at 10 km resolution.

3.2. EC-Earth

We used the output of atmosphere-only EC-Earth 2.3 (Hazeleger *et al* 2010) experiments at T799 (~25 km) described in detail in Haarsma *et al* (2013). There are four experiments of six ensemble members each: pre-industrial 1850–1854, present-day 2002–2006, near future 2030–2034 and end-of-century 2094–2098 (120 years total). The present-day experiment uses prescribed daily observationally-based reconstructions of sea surface temperatures (SST) at 0.25° resolution. The other experiments use the 2002–2006 observed SSTs transformed to the appropriate epoch by subtracting or adding the mean SST change of the ECHAM5/MPI-OM model used in the ESSENCE project with SRES A1B forcings (Sterl *et al* 2008) to the 2002–2006 conditions. Other boundary conditions, such as atmospheric greenhouse gas concentrations, were taken from the RCP4.5 scenario. This model has been shown to represent Atlantic hurricanes well in Haarsma *et al* (2013) and Baatsen *et al* (2015).

Figure 3. Observed maximum three-day averaged rainfall January–September 2017 (mm dy^{-1}). (*a*) GHCN-D v2 rain gauges, (*b*) CPC 25 km analysis, (*c*) NOAA calibrated radar (August 25–30 only), (*d*) NASA GPM/IMERG.

3.3. GFDL HiFLOR

As a second model, GFDL HiFLOR is used. HiFLOR is a fully coupled global climate model, based on GFDLs CM2.1 and CM2.5 (Delworth *et al* 2006, 2012). It uses a 25 km horizontal atmospheric and land grid, coupled to a coarser ocean and sea ice model. A detailed model description is provided in Murakami *et al* (2015) and van der Wiel *et al* (2016). Four static forcing experiments (1860, 1940, 1990, 2015) of variable length are available. The first 20 years of each integration are removed to allow for fast, near-surface ocean spin-up, and the remaining years concatenated to form a dataset that covers 565 years. Full details of the model experiments used are provided in van der Wiel *et al* (2017). The models are biased towards smaller precipitation extremes in the Gulf Coast region, though due to the relatively high resolution, this bias is significantly lower than in coupled models of average CMIP5 resolution (van der Wiel *et al* 2016).

The model data of HiFLOR are identical to the data that were used in van der Wiel *et al* (2017) because neither extensions to these experiments nor data over an extended region are publicly available at this time. However, the statistics along the coast are fairly constant (figure 2(*d*)), so the only problem arising when using a smaller box is that the probability for an event to occur anywhere on the coast is underestimated. In the observational gridded dataset, the return time for an event to occur in the larger box is about 25% lower than a similar event in the smaller box. However, the estimate of the change in return period or the changes in intensity due to anthropogenic climate change is not impacted by the size of the box after this bias correction. We have therefore chosen to include HiFLOR in this analysis, using the available model data.

3.4. Weather@home

The third model is the regional climate model (RCM) HadRM3P with ∼25 km horizontal resolution and 19 vertical levels (Massey *et al* 2015, Guillod *et al* 2017). The domain includes Central America, the United States, and the entire Gulf of Mexico region. Most modelled hurricanes affecting the Gulf Coast originate inside this domain. It is nested in and driven by the global HadAM3P model at N96 resolution. Three experiments are used in our analysis. (1) A 30 year climatology (1986–2015) with 30 simulations per year (= 900 members; ACTCLIM). (2) An actual ensemble with 1000 simulations for the August–October 2017 period (ACTUAL). (3) A natural or counterfactual ensemble with 1500 simulations for the August–October 2017 period (NATURAL). A smaller ensemble of ∼100 ACTUAL and NATURAL simulations is available for the February–July 2017 period. Lower
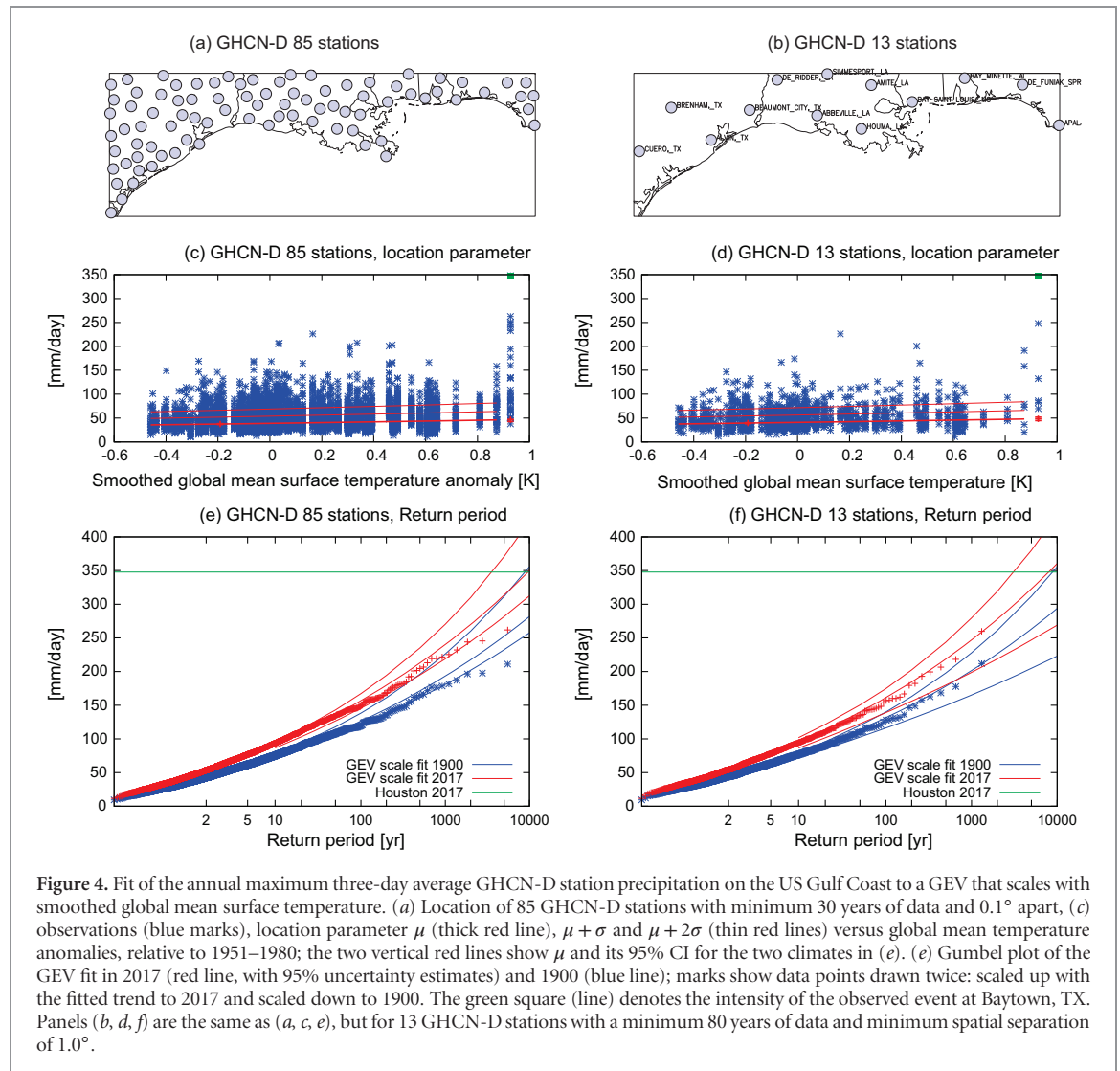
Figure 4. Fit of the annual maximum three-day average GHCN-D station precipitation on the US Gulf Coast to a GEV that scales with smoothed global mean surface temperature. (*a*) Location of 85 GHCN-D stations with minimum 30 years of data and 0.1° apart, (*c*) observations (blue marks), location parameter μ (thick red line), $\mu + \sigma$ and $\mu + 2\sigma$ (thin red lines) versus global mean temperature anomalies, relative to 1951–1980; the two vertical red lines show μ and its 95% CI for the two climates in (*e*). (*e*) Gumbel plot of the GEV fit in 2017 (red line, with 95% uncertainty estimates) and 1900 (blue line); marks show data points drawn twice: scaled up with the fitted trend to 2017 and scaled down to 1900. The green square (line) denotes the intensity of the observed event at Baytown, TX. Panels (*b, d, f*) are the same as (*a, c, e*), but for 13 GHCN-D stations with a minimum 80 years of data and minimum spatial separation of 1.0°.

boundary conditions are prescribed using OSTIA SSTs for ACTCLIM, and GloSea5 forecast SSTs for ACTUAL and NATURAL. ΔSSTs from CMIP5 historical and natural runs are used to obtain the naturalised SSTs (see Haustein *et al* (2016) for details). Forcings are prescribed according to the CMIP5 protocol (Meinshausen *et al* 2011).

3.5. Methods
Estimates of return periods and changes therein and changes in intensity are obtained with fits to GEVs that scale with the smoothed global mean temperature (GMST), inspired by the Clausius–Clapeyron relation. We investigated the alternative of using of SST averaged over the Gulf of Mexico, which would be more directly related to local atmospheric moisture content. The results this gives are very similar to those obtained using GMST, albeit with larger uncertainties due to the stronger noise in the local SST (from weather, local forcings and observational problems). Again, full details and the underlying assumptions are given in van der Wiel *et al* (2017).

Spatial dependencies are accounted for by a spatial moving block analysis as recommended by Efron

and Tibshirani (1998) for temporal dependencies. This technique was also used in Eden *et al* (2016) and van der Wiel *et al* (2017). The quality of the fits is checked by comparing the fit and observations for the current climate (red in subsequent plots) and a previous climate (blue in subsequent plots). We always quote two-sided 95% confidence intervals, which are estimated by a non-parametric bootstrap procedure.

4. Return periods and trends in observations

4.1. GHCN-D rain gauges
As mentioned before, for 2017, we take the observed value at Baytown (USC00410586) with 1043.4 mm 3dy^{-1}, corresponding to 347.8 mm dy^{-1}, over August 27–29. This is also the highest value observed in the box over all years. The 2017 event under study here is not included in the fits, although, of course, the 2016 Louisiana event is included.

In the larger station set of 85 stations (5193 station years, about 800 degrees of freedom), the return period of the 2017 three-day maximum in the current climate is more than 9000 yr (97.5% CI), figures 4(*a*), (*c*) and
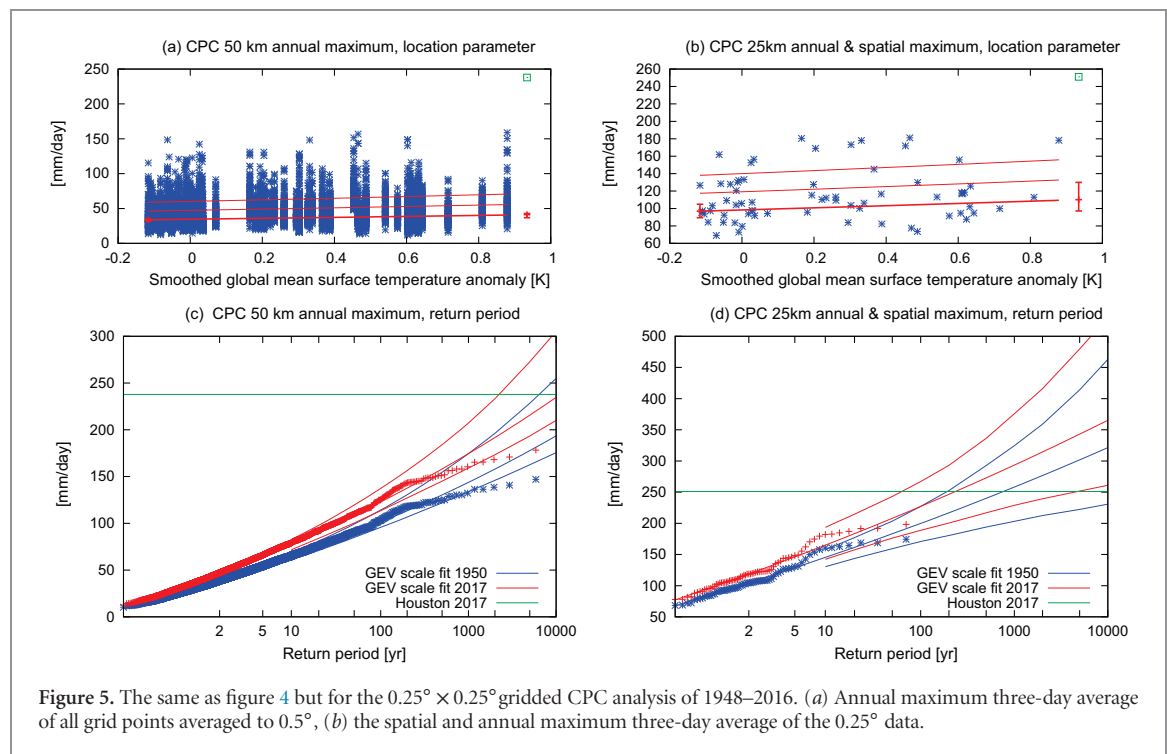
Figure 5. The same as figure 4 but for the 0.25° × 0.25° gridded CPC analysis of 1948–2016. (*a*) Annual maximum three-day average of all grid points averaged to 0.5°, (*b*) the spatial and annual maximum three-day average of the 0.25° data.

(*e*). The large extrapolation required makes the uncertainties large. This is a factor of four (2.1–5.0) larger than it was in the climate of 1900, corresponding to a 19% (12%–22%) increase in intensity.

This is confirmed by the fit to the much smaller dataset of 13 stations with at least 80 years of data and minimum distance 1° that are almost independent (1310 station years, about 1000 degrees of freedom), figures 4(*b*), (*d*) and (*f*). The GEV fit gives a return period of larger than 9000 yr in the current climate (97.5% CI), a factor of four (2.0–11) larger than in the climate of around 1900. The increase in intensity is also compatible: 18% (11%–25%).

We finally considered the spatial maximum in the box (not shown). For this, we use the 13-station dataset, which has a roughly constant number of stations between 1910 and 2010. A GEV fit over this period gives the return period for an event like this happening anywhere along the Gulf Coast between Corpus Christi, TX, and Apalachicola, FL. This is about once in 800 yr, with a 97.5% upper bound of less than once every 100 yr (i.e. less than a 1% probability every year). The risk ratio (RR), or the change in probability, has larger uncertainties in this measure than when using all stations. We find a value between 0.5 and 11.

4.2. CPC gridded analysis
As mentioned in section 3.1, we averaged the CPC gridded analysis to 0.5° to reduce the spatial dependencies. On this scale, the 2017 event is the highest in the dataset of 85 grid points (237.8 mm dy^{-1} or 9.36″ dy^{-1}), of which only five are independent. We find a return period for this much rain in a 50 km grid box of about 10 000 yr (2200–30 000 yr). Note that this likely an underestimate, as the rain radar gave higher

area averages. The probability in the current climate is a factor 5.4 (1.6–10) larger than in the climate of 1950, corresponding to an 18% (7%–24%) increase in intensity (figures 5(*a*) and (*c*)).

If we consider the annual and spatial maximum in the Gulf Coast region in the 0.25° dataset (251.1 mm dy^{-1} or 9.89″ dy^{-1}), this also shows an increase, albeit, again, with larger uncertainties (figures 5(*b*) and (*d*)). The return period of an extreme event like the one observed in 2017 or worse anywhere in the box is around 230 yr (60–5000 yr). The RR is very uncertain over this short time period: 3.2 (0.6–80) since 1950, corresponding to an increase in intensity of very roughly 12% (−5% to 29%).

We conclude from these two observational datasets that the probability of observed intense rainfall has increased by a factor of roughly four, very likely more than two, corresponding with an increase in intensity of about 20%, very likely more than 12%.

This was an extremely rare event given the past observations, even taking the trend into account. The return periods for a point observation as large as observed or larger is more than 9000 yr (97.5% CI). The chances of observing an event like this anywhere on the Gulf Coast are higher, but still low: less than 1 in 100 years (<1% yr^{-1}, 97.5% CI) for a point observation.

We show in the supplementary material available at stacks.iop.org/ERL/12/124009/mmedia that the probability in 2017 is not increased due to natural variability.

5. Attribution to anthropogenic factors

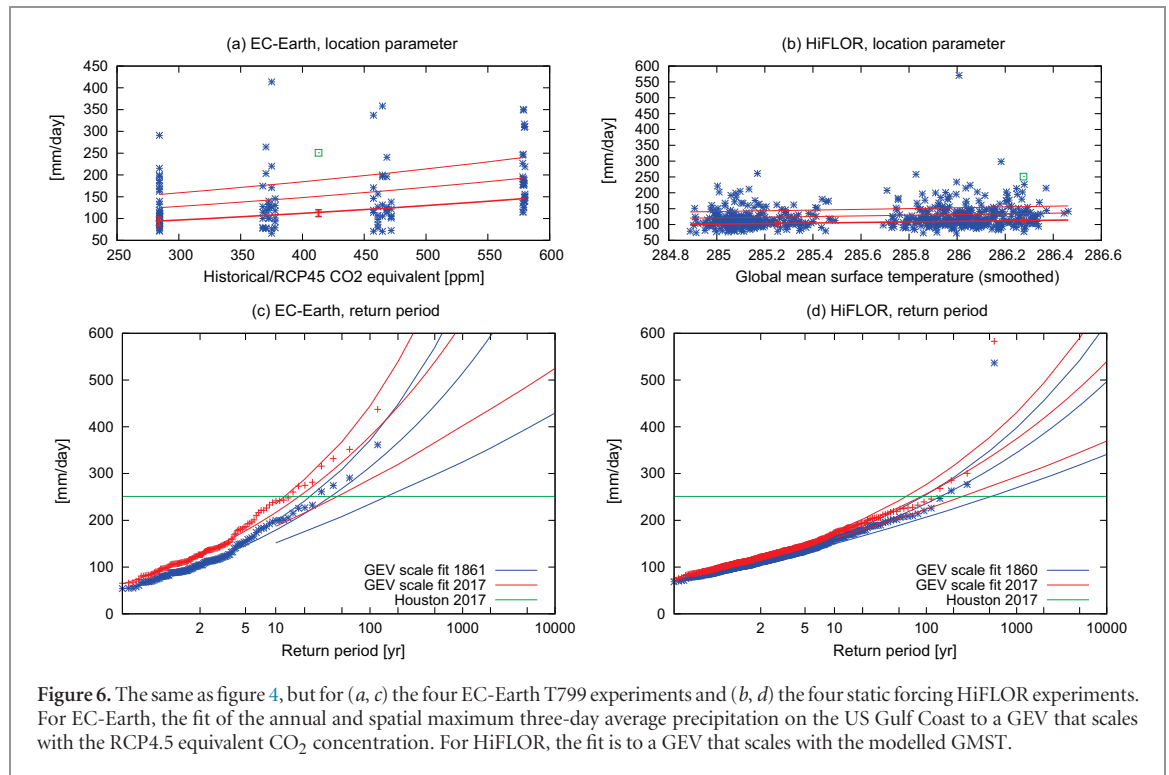To investigate the source of the observed increase, we have to use climate models in which we can study a

Figure 6. The same as figure 4, but for (*a, c*) the four EC-Earth T799 experiments and (*b, d*) the four static forcing HiFLOR experiments. For EC-Earth, the fit of the annual and spatial maximum three-day average precipitation on the US Gulf Coast to a GEV that scales with the RCP4.5 equivalent CO_2 concentration. For HiFLOR, the fit is to a GEV that scales with the modelled GMST.

counterfactual climate without anthropogenic influences, such as the emissions of greenhouse gases. As in van der Wiel *et al* (2017), we consider the spatial maximum over 27.5°N–31°N, 85°W–97.5°W of the annual maximum of three-day averaged precipitation. For HiFLOR, we could only use the somewhat smaller box 29°N–31°N, 85°W–95°W. This implies that there are fewer locations to reach the maximum precipitation. We correct the model output for this difference together with the bias correction.

5.1. Model evaluation

We investigated whether the models were fit for purpose in two ways: by comparing the tail of the extreme precipitation and the seasonal cycle of somewhat less extreme precipitation to the observations. The details are shown in the supplementary material. Based mainly on the shape of the tail, we decided to use the EC-Earth and GFDL models, but not the HadRM3P model.

5.2. EC-Earth

The extreme precipitation is fitted to a GEV that depends on the RCP4.5 equivalent CO_2 concentration, not the global mean temperature (figure 6(*a*)). This was done because there are no GMST observations for the two future periods and the CMIP5 RCP4.5 multi-model global mean temperature is not well-defined before 1860, as not all models simulate that period. The equivalent CO_2 concentration and multi-model global mean temperature are correlated at $r = 0.996$.

The GEV fit shows that the spatial maximum of the annual maximum of three-day precipitation along the Gulf Coast is simulated reasonably well (figure 6(*c*)), although due to the high scale parameter σ (steeper
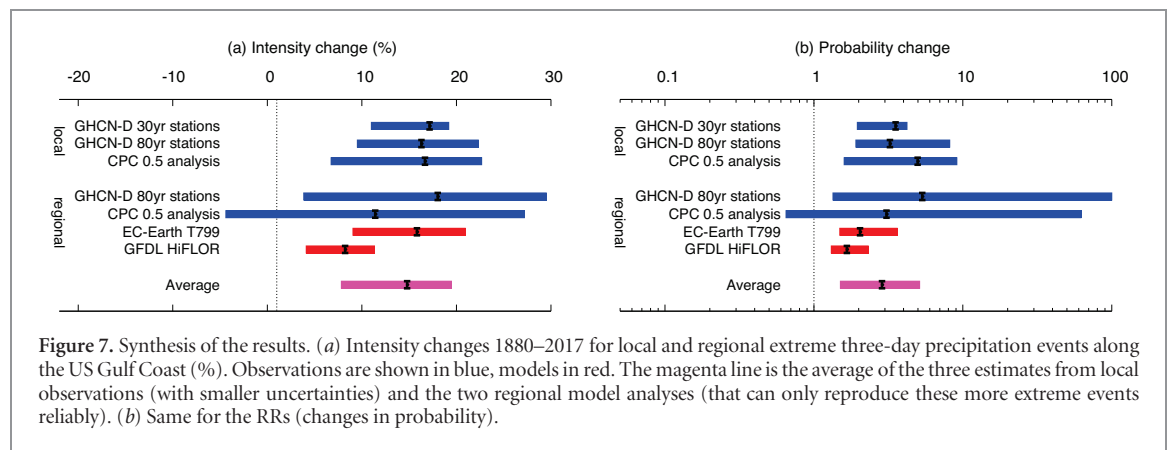
slope), the return period is lower than in the observations (figure 5(*d*)). The fit assumes that the scaling up to 2100 is the same as up to 2017. It gives an increase in intensity from of 1861–2017 of 17% (10%–23%), corresponding to an increase in probability of a factor 2.2 (1.5–4.1).

5.3. HiFLOR

As mentioned in the supplementary material, the GEV fits provide a multiplicative bias correction of 80% to correct for the modelled extremes that are smaller than observed and the difference in box sizes (see section 3.3). The model bias over the same box is about 40%. The return period is compatible with the observed one, as expected after bias correction. The increase in probability (RR) is 1.6 with a 95% CI of 1.3–2.3. This corresponds to an increase in intensity of 8% (4%–11%, figures 6(*b*) and (*d*)).

6. Synthesis

Figure 7 summarises the results obtained above. The top three results show the changes for local extremes, i.e. for an event to occur at a specific location. The next four show the changes in the spatial maximum, i.e. for an event to occur anywhere along the US Gulf Coast. The latter fits involve only the most extreme events, giving $\mathcal{O}(10)$ times fewer degrees of freedom. The uncertainties due to natural variability are therefore larger, but the two models that passed the evaluation can only reproduce these most extreme events reliably. In the observations, the regional extremes are smoothly connected to less extreme events, so we can use the changes in the local extremes to deduce the changes

Figure 7. Synthesis of the results. (*a*) Intensity changes 1880–2017 for local and regional extreme three-day precipitation events along the US Gulf Coast (%). Observations are shown in blue, models in red. The magenta line is the average of the three estimates from local observations (with smaller uncertainties) and the two regional model analyses (that can only reproduce these more extreme events reliably). (*b*) Same for the RRs (changes in probability).

in the regional extremes. We therefore compute the last line as the unweighted average of the three estimates for changes in local extremes from observational datasets and the two estimates from models for changes in regional extremes.

It should be noted that changes at the return period of the extreme rainfall from Hurricane Harvey in 2017, estimated at more than 9000 yr from the station data, can only be deduced from a GEV fit to the various datasets by assuming the properties do not change in the extrapolation from the more common extreme events, as none of the models has enough data to sample this probability directly.

Both the observations and EC-Earth show an increase in intensity ΔI of around 16% per degree global warming (figure 7(*a*)). As this part of the Gulf of Mexico and the Gulf Coast have warmed by about the same amount as the global mean, this is equivalent to two times Clausius–Clapeyron scaling. In contrast, the HiFLOR model only shows an increase of about 8%, which is more compatible with $1\times$CC scaling. The spread in results is not compatible within natural variability, $\chi^2/\mathrm{dof}\approx 4$ for the two datasets and two model results, so there are systematic differences between the models that must be taken into account.

The same picture appears for the RRs (figure 7(*b*)); again, the EC-Earth results are in line with the observations (in spite of the too high variability). Extreme rainfall on the Gulf Coast in HiFLOR is less sensitive to global warming than EC-Earth in this region.

We conclude that precipitation extremes on the US Gulf Coast have increased due to global warming. The increase is higher in the observations ($12 < \Delta I < 22\%$) and one of the two models ($10 < \Delta I < 23\%$) than in the other model ($4 < \Delta I < 11\%$). Both should include possible stalling effects. If the station observations are homogeneous enough, this points to $2\times$CC scaling. However, there may be inhomogeneities in the observations (well after 1948) that could cause an overestimation of the trend, which would imply somewhat lower scaling. The unweighted average of the local change in intensity in three relatively independent observational datasets and the regional change

in the two models gives an increase of 15% with an uncertainty range 8%–19%.

These increases are equivalent to an increase in probability of at least a factor two in the observations, somewhat less in the models. An unweighted average on a logarithmic scale gives a most likely increase of a factor of 3, with uncertainty range of 1.5–5.

Extrapolating these trends to the future, we expect another similar increase if global warming is limited to 2 °C above pre-industrial levels. However, under a 'business-as-usual' scenario in which the world continues to rely primarily on fossil fuels, the intensity of extreme rainfall events on the Gulf Coast would increase by about 50% as the world warms another four degrees. This corresponds to an increase in probability of a factor of roughly 10 (both numbers have large uncertainties). This is in rough agreement with the increase of a factor of 18 that Emanuel (2017) finds relative to 1981–2000 for large-area averaged precipitation (their value for 2017 is larger than ours mainly due to the linear interpolation rather than the exponential one we use).

7. Vulnerability and exposure

While this study focuses on the rainfall hazard, the primary impact was flooding. Drivers that exacerbate or reduce impacts in storms of this scale are a complex combination of an extreme natural hazard, long-term planning decisions and short term disaster preparedness and response decisions. These are discussed in detail in the supplementary material. Although the extreme rainfall levels from Hurricane Harvey are extremely rare, additional factors, such as rapid population growth, urban growth policies, and ageing water management infrastructure further exacerbate the ultimate impacts of this storm. Recent flood events resulting from storms such as Tropical Storm Allison (2001), Hurricane Ike (2008), Memorial Day (2015), and Tax Day (2016) further illustrate the importance of managing exposure and vulnerability when reducing the level of flood impacts in Houston.

8. Conclusions

As described in the introduction and methods, this study has focused primarily on the changes in extreme rainfall in the US Gulf Coast region, applied to the rainfall during Hurricane Harvey that caused record flooding in Houston. The first result is that the three-day rainfall sums that were responsible for most of the flooding were extremely rare, with a return time for station observations of more than 9000 yr (97.5% CI) in the current climate, taking the trend into account. This would have caused flooding in any city.

The second result is that we find strong evidence that global warming over the last century, primarily caused by anthropogenic greenhouse gas emissions, has increased the intensity of the three-day rainfall extremes on the Gulf Coast, or equivalently, has increased the probability of a given rainfall event. Due to the rarity of the observed rainfall in Houston, applying the increase observed for less extreme events to this event requires a (reasonable) extrapolation. We find that the intensity of rainfall increased by 15% (8%–19%) and the probability of this much rain or more by a factor of three (1.5–5). This increase in rainfall intensity contributed to the flooding observed in Houston and surrounding areas. Less extreme rainfall events have also resulted in impactful flooding in Houston in previous years, and their return times are also decreasing.

We also acknowledge that several other factors have likely also contributed to increased flood risk in Houston over the past century and should be further explored. First, given Houston's proximity to the coast, relative sea level rise has likely contributed to increases in flood risk in the region. While NOAA estimates that sea level rise near Galveston Island is increasing by approximately 6.47 mm yr^{-1}, further analysis is required to disentangle the relative contributions of anthropogenic climate change and regional subsidence to increases in sea levels in Galveston Bay and their effects on flood risk in Houston. Second, the effects of regional changes in land use and land cover on flooding during Hurricane Harvey, as well as the long-term performance and operation of flood adaptation measures employed in Houston, are of interest and importance to local governing bodies. Finally, additional research is required to determine to what extent Harvey's storm surge contributed to compound flooding in coastal watersheds, and whether compound flooding during tropical cyclones should be considered in the design of coastal flood defences.

While these questions were not answered in this study, our results provide one of the big pieces of the puzzle showing that although rainfall during Hurricane Harvey was exceptional, the trend in extreme rainfall needs to be taken into account when considering upgrades to flood infrastructure in Houston and surrounding areas since additional global warming will continue to increase the risk of extreme precipitation events further.

ORCID iDs

Geert Jan van Oldenborgh ⓘ https://orcid.org/0000-0002-6898-9535
Friederike Otto ⓘ https://orcid.org/0000-0001-8166-5917
Sihan Li ⓘ https://orcid.org/0000-0002-2479-8665
Karin van der Wiel ⓘ https://orcid.org/0000-0001-9365-5759
Gabriel Vecchi ⓘ https://orcid.org/0000-0002-5085-224X
Antonia Sebastian ⓘ https://orcid.org/0000-0002-4309-2561
Julie Arrighi ⓘ https://orcid.org/0000-0003-4714-4514
Heidi Cullen ⓘ https://orcid.org/0000-0002-6976-2631
Karsten Haustein ⓘ https://orcid.org/0000-0003-3126-7851

References

Baatsen M, Haarsma R J, Van Delden A J and de Vries H 2015 Severe autumn storms in future western Europe with a warmer Atlantic Ocean *Clim. Dyn.* **45** 949–64

Brody S D, Zahran S, Highfield W E, Grover H and Vedlitz A 2008 Identifying the impact of the built environment on flood damage in Texas *Disasters* **32** 1–8

Brody S D, Blessing R, Sebastian A and Bedient P 2011 Examining the impact of land use/land cover characteristics on flood losses *J. Environ. Plan. Manage.* **57** 1252–65

Clapeyron E 1834 Mémoire sur la puissance motrice de la chaleur *Journal de l'Ecole Royale Polytechnique* **XIV** 153–90

Clausius R 1850 Ueber die bewegende Kraft der Wärme und die Gesetze, welche sich daraus für die Wärmelehre selbst ableiten lassen *Annalen der Physik* **155** 368–97

Delworth T L *et al* 2006 GFDL's CM2 global coupled climate models. Part I: formulation and simulation characteristics *J. Clim.* **19** 643–74

Delworth T L *et al* 2012 Simulated climate and climate change in the GFDL CM2.5 high-resolution coupled climate model *J. Clim.* **25** 2755–81

Eden J M, Wolter K, Otto F E L and van Oldenborgh G J 2016 Multi-method attribution analysis of extreme precipitation in Boulder, Colorado *Environ. Res. Lett.* **11** 124009

Efron B and Tibshirani R J 1998 *An Introduction to the Bootstrap* (New York: Chapman and Hall)

Emanuel K 2017 Assessing the present and future probability of Hurricane Harvey's rainfall *Proc. Natl Acad. Sci.* **114** 12681–84

FEMA 2017 Historic Disaster Response to Hurricane Harvey in Texas (www.fema.gov/news-release/2017/09/22/historic-disaster-response-hurricane-harvey-texas)

Guillod B P *et al* 2017 Weather@home 2: validation of an improved global–regional climate modelling system *Geosci. Model Dev.* **10** 1849–72

Haarsma R J, Hazeleger W, Severijns C, de Vries H, Sterl A, Bintanja R, van Oldenborgh G J and van den Brink H W 2013 More hurricanes to hit western Europe due to global warming *Geophys. Res. Lett.* **40** 1783–88

Haustein K, Otto F E L, Uhe P, Schaller N R A M, Hermanson L, Christidis N, McLean P and Cullen H 2016 Real-time extreme weather event attribution with forecast seasonal SSTs *Environ. Res. Lett.* **11** 064006

Hazeleger W *et al* 2010 EC-Earth: a seamless Earth-system prediction approach in action *Bull. Am. Meteorol. Soc.* **91** 1357–63

Held I M and Soden B J 2006 Robust responses of the hydrological cycle to global warming *J. Clim.* **19** 5686–99

Hesselbjerg Christensen J *et al* 2013 Climate phenomena and their relevance for future regional climate change *Climate Change 2013: The Physical Science Basis* ed T F Stocker *et al* (Cambridge: Cambridge University Press) ch 14 pp 1217–1308

Hoerling M P, Wolter K, Perlwitz J, Quan X, Eischeid J, Wang H, Schubert S, Diaz H F and Dole R M 2013 Northeast Colorado extreme rains interpreted in a climate change context *Bull. Am. Meteorol. Soc.* **95** S15–18

Knutson T R, Mcbride J I, Chan J, Emanuel K, Holland G, Landsea C W, Held I M, Kossin J P, Srivastava A K and Sugi M 2010 Tropical cyclones and climate change *Nat. Geosci.* **3** 157–63

Knutson T R, Sirutis J J, Vecchi G A, Garner S, Zhao M, Kim H-S, Bender M, Tuleya R E, Held I M and Villarini G 2013 Dynamical downscaling projections of twenty-first-century Atlantic hurricane activity: CMIP3 and CMIP5 model-based scenarios *J. Clim.* **26** 6591–6617

Lenderink G, Barbero R, Loriaux J M and Fowler H J 2017 Super-Clausius–Clapeyron scaling of extreme hourly convective precipitation and its relation to large-scale atmospheric conditions *J. Clim.* **30** 6037–52

Mann M E, Rahmstorf S, Kornhuber K, Steinman B A, Miller S K and Coumou D 2017 Influence of anthropogenic climate change on planetary wave resonance and extreme weather events *Sci. Rep.* **7** 45242

Massey N, Jones R, Otto F E L, Aina T, Wilson S, Murphy J M, Hassell D, Yamazakif Y H and Allen M R 2015 Weather@home | development and validation of a very large ensemble modelling system for probabilistic event attribution *Q. J. R. Meteorol. Soc.* **141** 1528–45

Meinshausen M *et al* 2011 The RCP greenhouse gas concentrations and their extensions from 1765–2300 *Clim. Change* **109** 213

Murakami H *et al* 2015 Simulation and prediction of category 4 and 5 hurricanes in the high-resolution GFDL HiFLOR coupled climate model *J. Clim.* **28** 9058–79

NOAA NCEI 2017 Billion-Dollar Weather and Climate Disasters: Overview (www.ncdc.noaa.gov/billions)

O'Gorman P A 2015 Precipitation extremes under climate change *Current Clim. Change Rep.* **1** 49–59

Schumacher R S and Johnson R H 2006 Characteristics of US extreme rain events during 1999–2003 *Weath. Forecast.* **21** 69–85

Scoccimarro E, Gualdi S, Villarini G, Vecchi G A, Zhao M, Walsh K and Navarra A 2014 Intense precipitation events associated with landfalling tropical cyclones in response to a warmer climate and increased CO_2 *J. Clim.* **27** 4642–54

Sebastian A, Dupuits E J. C and Morales-Nápoles O 2017 Applying a Bayesian network based on Gaussian copulas to model the hydraulic boundary conditions for hurricane flood risk analysis in a coastal watershed *Coast. Eng.* **125** 42–50

Sterl A, Severijns C, Dijkstra H, Hazeleger W, van Oldenborgh G J, van den Broeke M, Burgers G, van den Hurk B, van Leeuwen P J and van Velthoven P 2008 When can we expect extremely high surface temperatures? *Geophys. Res. Lett.* **35** L14703

Torres J, Bass B, Irza N, Fang Z, Proft J, Dawson C, Kiani M and Bedient P 2015 Characterizing the interactions of hurricane storm surge and rainfall-runoff for the Houston-Galveston region *Coast. Eng.* **106** 7–19

van der Wiel K, Kapnick S B, Vecchi G A, Cooke W F, Delworth T L, Jia L, Murakami H, Underwood S and Zeng F 2016 The resolution dependence of contiguous US precipitation extremes in response to CO_2 forcing *J. Clim.* **29** 7991–8012

van der Wiel K, Kapnick S B, van Oldenborgh G J, Whan K, Philip S, Vecchi G A, Singh R K, Arrighi J and Cullen H 2017 Rapid attribution of the August 2016 flood-inducing extreme precipitation in south Louisiana to climate change *Hydrol. Earth Syst. Sci.* **21** 897–921

Vecchi G A and Knutson T R 2011 Estimating annual numbers of Atlantic hurricanes missing from the HURDAT database (1878–1965) using ship track density *J. Clim.* **24** 1736–46

Villarini G, Lavers D A, Scoccimarro E, Zhao M, Wehner M F, Vecchi G A, Knutson T R and Reed K A 2014 Sensitivity of tropical cyclone rainfall to idealized global-scale forcings *J. Clim.* **27** 4622–41

Westra S, Alexander L V and Zwiers F W 2012 Global increasing trends in annual maximum daily precipitation *J. Clim.* **26** 3904–18